4. V.I. Emel'yanov, "Defect-deformational surface roughening and melting and giant enhancement of optical processes at surface of solids," Laser Physics **8**, 937–940 (1998).
5. J.S. Preston, H.M. van Driel, J.E. Sipe, "Pattern formation during laser melting of silicon," Phys. Rev. B **40**, 3942–3954 (1989).

CTuA14

Engineering of effective quadratic and cubic nonlinearities in two-period QPM gratings

O. Bang, C.B. Clausen,* Lluis Torner,**
Department of Mathematical Modelling, Technical Univ. of Denmark, Bldg. 305, 2800 Kongens Lyngby, Denmark; E-mail: ob@imm.dtu.dk.

Quasi-phase-matching (QPM) by electric-field poling in ferro-electric materials, such as $LiNbO_3$, is promising due to the possibilities of engineering the photolithographic mask, and thus the QPM grating, without also generating a linear grating. A proper design of the longitudinal grating structure allows for distortion free temporal pulse compression,[1] soliton shaping,[2] broad-band phase matching,[3] multi-wavelength second-harmonic generation (SHG),[4] and an enhanced cascaded phase shift.[5] Transverse patterning can be used for beam-tailoring,[6] broad-band SHG[7] and soliton steering.[8]

At lowest order the effect of QPM is to eliminate the phase mismatch and average the quadratic (or $\chi^{(2)}$) nonlinearity, resulting in an effective $\chi^{(2)}$ nonlinearity experienced by the slowly-varying (on the scale of the coherence length) averaged field, which is reduced by a factor of $\pi/2$. At the next order QPM induces cubic nonlinear self- and cross-phase modulation terms in the equations for the averaged field.[9] This induced nonlinearity is a result of non-phase-matched coupling between the average field and higher order modes[10] and of a fundamentally different nature than the intrinsic material Kerr nonlinearity. So far it was shown how the induced $\chi^{(3)}$ nonlinearity affects the amplitude and phase modulation of cw waves,[11] while still supporting solitons.[9] However, in conventional materials with single period QPM the cubic corrections were small. Here we show analytically and verify numerically how the average $\chi^{(2)}$ and $\chi^{(3)}$ nonlinearities can be engineered by modulating the QPM grating, such as, e.g., to make their effects equally strong.

We consider a linearly polarized electric field $\vec{E} = \hat{e}[E_1(z)\exp(ik_1z - i\omega t) + E_2(z)\exp(ik_2z - i2\omega t) + c.c.]/2$, propagating in a lossless QPM $\chi^{(2)}$ medium under conditions for type I SHG. Then the dynamical equations take the form

$$i\frac{dE_1}{dz} + G(z)\chi_1E_1^*E_2e^{-i\Delta kz} = 0,$$

$$i\frac{dE_2}{dz} + G(z)\chi_2E_1^2e^{i\Delta kz} = 0, \qquad (1)$$

where $\chi_j = \omega d_{\rm eff}/(n_jc)$, $E_1(z)$ is the slowly varying envelope of the fundamental wave (FW)

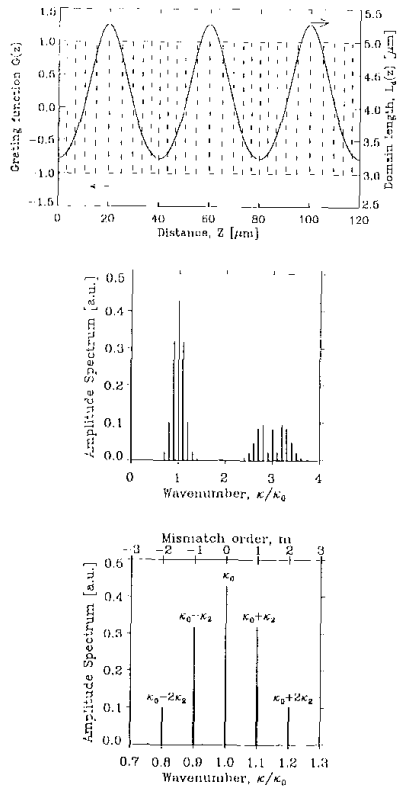

CTuA14 Fig. 1. Left: Modulated QPM grating function $G(z)$ (left, dotted) with the corresponding local domain length $L_d(z)$ (right, solid) for $L_2 = 10L_0 = 40$ μm and $\varepsilon_2 = 1.2$. Center: Amplitude spectrum of $G(z)$ for $\varepsilon_2 = 1.2$ and $L_2 = 20L_0 = 100$ μm. Right: Block structure around $\kappa = \kappa_0$ with indication of the order m of the effective mismatch β_m.

with frequency ω, refractive index n_1, and wavevector k_1, and $E_2(z)$ is the second harmonic (SH) with refractive index n_2 and wavevector k_2 ($j = 1,2$). The $\chi^{(2)}$ coefficient $d_{\rm eff} = [\chi^{(2)}]/2$ is given in MKS units, and $\Delta k = 2k_1 - k_2$ is the wavevector mismatch. The modulation of the $\chi^{(2)}$ susceptibility is described by the periodic grating function $G(z)$ with unit amplitude and Fourier series $G(z) = \sum_n g_n \exp[inf(z)]$, where g_n are the coefficients of the unperturbed square grating. We take $f(z) = \lambda_0 z + \varepsilon_2 \sin(\lambda_2 z)$ and consider weakly modulated QPM gratings with $L_2/\varepsilon_2 \gg L_0$, where $L_2 = 2\pi/\lambda_2$ is the modulation period and $L_0 = \pi/\lambda_0$ is the unperturbed domain length. This corresponds to a two-period square grating with a periodic slowly varying local domain length given by $L_d(z) = \pi/[\lambda_0 + \varepsilon_2K_2\cos(K_2z)]$, as illustrated in Fig. 1 (left).

Following the approach of[9] we obtain the average fields on the shortest scale of $L_0 \ll L_2$, with a modulated effective $\chi^{(2)}$ nonlinearity that depends on z. Assuming that the modulation length is still much shorter than the crystal length, $L_2 \ll L$, the spectrum of $G(z)$ has the block structure shown in Fig. 1 (center), which allows us to do a second independent averaging on the L_2-scale. Thus we obtain the final equations for the average fields, which includes the induced cubic nonlinear terms:

$$i\frac{dw}{dz} + \eta_{1m}w^*ve^{-i\beta_mz} + (\gamma_{2m}|w|^2 - \gamma_{1m}|v|^2)w = 0,$$

$$i\frac{dv}{dz} + \eta_{m1}w^2e^{i\beta_mz} - 2\gamma_{2m}|w|^2v = 0, \qquad (2)$$

where $\beta_m = \beta_0 - mk_2 = \Delta k - \kappa_0 - m\kappa_2 \ll \kappa_2$ is the effective mismatch for matching to the mth peak next to the κ_0 peak, as illustrated in the close-up in Fig. 1 (right). The nonlinearity coefficients are given by

$$\eta_{jm} = \chi_j[2J_m(\varepsilon_2)/\pi],$$
$$\gamma_{jm} = \chi_1\chi_j[(\pi^2 - 8)/\kappa_0 - 4S_m(\varepsilon_2)/\kappa_2]/\pi^2, \qquad (3)$$

where $S_m = -S_{-m} = -\sum_{n\neq 0}J_n+m2/\eta$, with $S_0 = 0$ and $S_1 = -2J_0(\varepsilon_2)J_1(\varepsilon_2)/\varepsilon_2$.

Using the averaged Eqs. (2), which were recently derived and studied analytically in Ref. [12], we focus on $LiNbO_3$ and study the competition between the effective $\chi^{(2)}$ and $\chi^{(3)}$ nonlinearities. We show how the induced average $\chi^{(3)}$ nonlinearity can dominate the intrinsic material one, thereby decreasing the intensity at which the $\chi^{(2)}$ and $\chi^{(3)}$ effects balance and compete to a few GW/cm^2. The analytical model is confirmed numerically and the implications for the bandwidth of SHG is studied.

The authors acknowledge support from the Danish Technical Research Council (Talent Grant no. 9800400).

*AT&T Res. Labs., USA
**Univ. Politecnica de Catalunya, Spain

1. M.A. Arbore, O. Marco, M.M. Fejer, "Pulse compression during second-harmonic generation in aperiodic quasi-phase-matched gratings," Opt. Lett. **22**, 865 (1997); M.A. Arbore, A. Galvanauskas, D. Harter, M.H. Chou, M.M. Fejer, "Engineerable compression of ultrashort pulses by use of second-harmonic generation in chirped-period-poled lithium niobate," Opt. Lett. **22**, 1341 (1997).
2. L. Torner, C. Balslev Clausen, M.M. Fejer, "Adiabatic shaping of quadratic solitons," Opt. Lett. **23**, 903 (1998).
3. K. Mizuuchi and K. Yamamoto, "Waveguide second-harmonic generation device with broadened flat quasi-phase-matching response by use of a grating structure with located phase shifts," Opt. Lett. **23**, 1880 (1998).
4. S. Zhu, Y. Zhu, Y. Qin, H. Wang, C. Ge, N. Ming, "Experimental realization of second-harmonic generation in a Fibonacci optical superlattice of $LiTaO_3$," Phys. Rev. Lett. **78**, 2752 (1997).
5. M. Cha, "Cascaded phase shift and intensity modulation in aperiodic quasi-phase-matched gratings," Opt. Lett. **23**, 250 (1998).
6. G. Imeshev, M. Proctor, M.M. Fejer, "Lateral patterning of nonlinear frequency conversion with transversely varying quasi-phase-matching gratings," Opt. Lett. **23**, 673 (1998).
7. P.E. Powers, T.J. Kulp, S.E. Bisson, "Continuous tuning of a continuous-wave periodically poled lithium niobate optical parametric oscillator by use of a fan out grating design," Opt. Lett. **23**, 159 (1998).

8. C. Balslev Clausen, L. Torner, "Self-bouncing of quadratic solitons," Phys. Rev. Lett. **81,** 790 (1998); "Spatial switching of quadratic solitons in engineered quasi-phase-matched structures," Opt. Lett. **24,** 7 (1999).
9. C. Balslev Clausen, O. Bang, Y.S. Kivshar, "Spatial solitons and induced Kerr effects in quasi-phase-matched quadratic media," Phys. Rev. Lett. **78,** 4749 (1997).
10. O. Bang, Y.S. Kivshar, A.V. Buryak, A. De Rossi, S. Trillo, "Two-dimensional solitary waves in media with quadratic and cubic nonlinearity," Phys. Rev. E **58,** 5057 (1998).
11. A. Kobyakov, F. Lederer, O. Bang, Y.S. Kivshar, "Nonlinear phase shift and all-optical switching in quasi-phase-matched quadratic media," Opt. Lett. **23,** 506 (1998).
12. O. Bang, C. Balslev Clausen, P.L. Christiansen, L. Torner, "Engineering competing nonlinearities," Opt. Lett. **24,** 1413 (1999).

CTuA15

Generation of <4 cm^{-1} transform-limited pulses in IR by difference frequency mixing of stretched pulses

G. Veitas, R. Danielius, E. Schreiber,* *Laser Research Center, Vilnius Univ., Sauletekio Avenue 9, Building 3, 2040 Vilnius, Lithuania; E-mail: gediminas.veitas@ff.vu.lt*

In our previous paper we have presented the theoretical background and experimental verification of narrow-bandwidth pulse generation via difference frequency mixing.[1] The tunability of generated narrow-bandwidth pulses was restricted to rather narrow wavelength range in the proximity of 1 μm, which is not of great practical interest.

In the present contribution, we report on generation of narrow-bandwidth pulses within a 3–5 μm wavelength region that can be applied to highly selective time-resolved vibrational spectroscopy.

As a pump source we used a picosecond Ti:Sapphire laser system delivering 800-nm-wavelength pulses with duration of 1.8 ps and energy of 1.5 mJ. A part of the laser output was frequency doubled and used to pump an optical parametric generator-amplifier (OPO/A), which produced ~1.3-ps pulses in 470–2600-nm-wavelength range. The idler wave of the OPO/A was used as a seed for subsequent difference frequency (DF) mixing/parametric amplification pumped by 800-nm pulses.

In the first series of experiments we generated the difference frequency in a conventional way. Laser and seed pulses were mixed in a 7-mm-thick KTA crystal without stretching. The DF pulses that were produced had a bandwidth of 12.3 cm^{-1} (Fig. 1).

We measured duration of amplified seed pulse to be 1.2 ps (Fig. 2). Computer simulation of the process has shown that both DF pulse and amplified seed have similar duration when group velocity mismatch is as small as in our case. With this assumption we estimate the time-bandwidth product of the IR pulses to be ~0.43, which is very close to the time-bandwidth product of transform-limited Gaussian pulses. We measured the IR pulse energy of 70 μJ at 3 μm and 25 μJ at 5 μm, with pump pulse energy of 1.2 mJ.

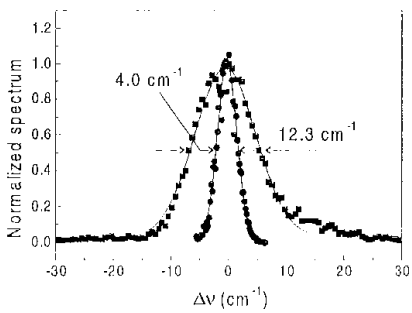

CTuA15 Fig. 1. Spectrum profiles of conventional (squares) and narrow-bandwidth (circles) difference frequency pulses.

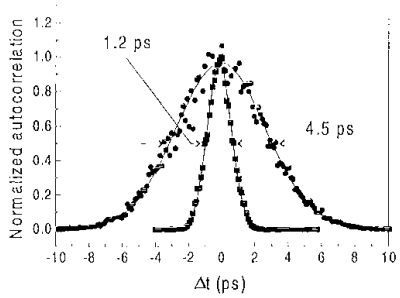

CTuA15 Fig. 2. Autocorrelation traces of amplified idler pulses in conventional (squares) and narrow-bandwidth (circles) difference frequency mixing.

In the second set of experiments, pump and seed pulses were stretched in two separate grating stretchers to ~8-ps duration. The stretcher for the pump pulses was fixed whereas that for the seed had adjustable grating incidence angle, stretcher length and automatic delay compensation. The pulses were mixed in a 15-mm-thick KTA crystal. The bandwidth of generated DF pulse was a function of the seed stretcher length and had a minimum at the point where the chirp of pump and seed was calculated to be equal.[1] The narrowest DF bandwidth of 3 cm^{-1} was observed at 3 μm. The pulses at longer wavelengths had a bandwidth of ~4 cm^{-1} (Fig. 1). Duration of the amplified seed pulse was measured to be 4.6 ps (Fig. 2). Again, according to computer simulation the amplified seed and IR pulses have nearly the same duration. With this assumption we again estimate the time-bandwidth product of the IR pulses to be 0.4–0.5. With the pump energy at the DFG stage of 550 μJ the energy of generated IR pulse ranged from 3 μJ at 5 μm to 35 μJ at 3 μm.

In conclusion, we have generated transform-limited pulses of <4-cm^{-1} bandwidth, tunable in the range of 3–5 μm. Further extension of the tuning range requires pump wavelengths longer than 800 nm since existing IR transparent crystals exhibit one- and/or two-photon absorption, which results not only in energy loss but also in heavy thermal lensing.

*Princeton Univ., USA

1. G. Veitas and R. Danielius, "Generation of narrow-bandwidth tunable picosecond pulses by difference-frequency mixing of stretched pulses," J. Opt. Soc. Am. B **16,** 1561–1565 (1999).

CTuA16

Thermally stable third harmonic generation using type 1 LBO

K. Deki, T. Yokota, J. Sakuma, Y. Ohsako, *Ushio Res. Inst. of Tech. Inc., Gotenba R&D Lab., 1-90 Komakado Gotenba-shi, Shizuoka-Ken, 412-0038 Japan; E-mail: dekikic@mail.ushio.co.jp*

The third-harmonic light sources of Nd:YAG/YLF lasers have begun to be utilized for drilling via holes in print circuit boards according to the progress of high-density fabrication. Fast rise-time in burst mode operation and high pulse energy stability are required for the light source in this industrial use. Because of simple construction and less optical component requirement, type 1 SHG-type 2 THG(LBO) scheme has often been used for the third-harmonic generation. However it has unstable rise-time property in high average power op-

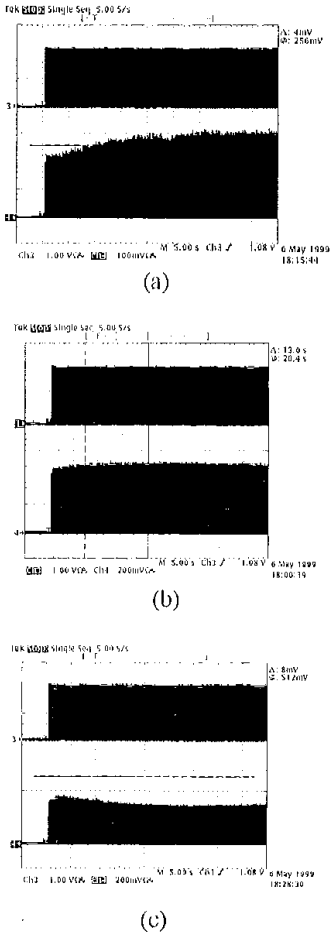

CTuA16 Fig. 1. The fundamental and THG output waveforms for type 2 THG LBO. Crystal temperature is 49, 50, and 51°C, respectively.